Research article

Silicon microsurgery-force sensor based on diffractive optical MEMS encoders

Xiaojing Zhang

The author

Xiaojing Zhang is based at the Department of Electrical Engineering, Stanford University, USA.

Keywords

Force measurement, Sensors, Optical instruments, Microsurgery

Abstract

This paper presents a micrograting-based force sensor integrated with a surface micromachined silicon-nitride probe suitable for characterizing microsurgery force on a single cell or embryo. The probe is supported by springs of a known spring constant, and the surgical penetration force is determined from displacement measurements. The optical-encoder force sensor exhibits configurable sensitivity and dynamic range, allowing monitoring over a wide range of forces. The periodicity of the encoder response can be used for calibration of the injector displacement and to obtain information about the localized elastic properties of the target. We used a force sensor with a measured spring constant of 1.85 N/m for penetration force measurements on Drosophila embryos, and found a penetration force of 52.5 μN (± 13.2 percent) and a membrane displacement of 58 μm (± 5.2 percent).

Electronic access

The Emerald Research Register for this journal is available at
www.emeraldinsight.com/researchregister

The current issue and full text archive of this journal is available at
www.emeraldinsight.com/0260-2288.htm

Sensor Review
Volume 24 · Number 1 · 2004 · pp. 37–41
 · ISSN 0260-2288
DOI 10.1108/02602280410515806

Localized and accurate microsurgery for trans-membrane delivering genetic material into biological model systems, such as Drosophila, will enable a variety of studies of developmental biology and genetics including RNA interference (RNAi) (Sharp and Zamore, 2000). For such studies to be carried out *in vivo*, the damage caused by the penetration must be minimized. Silicon's material properties, together with established micromachining technology, make it ideal for microsurgical tools. A bulk-machined silicon needle with centimeter scale suitable for dissecting human eye cataractous lens was demonstrated in mid-1990s (Lal and White, 1995), however, without real-time quantification of cutting force. We have developed 10^3 times down-scaled surface micromachined silicon-nitride needles (Zappe *et al.*, 2002) with integrated force sensors for measurements of the static penetration force into Drosophila embryo (Zhang *et al.*, n.d.; Zhang *et al.*, 2003).

The force sensor is an optical encoder based on transmission phase gratings integrated with the needle. Any diffraction grating can be characterized into either amplitude grating or phase grating based on its transmission function (Figure 1), which is in general complex, since both the amplitude and phase of the light may be altered on passing through the object. The amplitude grating has a transmission function that varies in amplitude within the aperture. A phase grating modifies only the phase of an incoming wave (atleast to a first approximation, not the amplitude). Phase gratings are advantageous in transmission because of their high optical throughput compared to amplitude gratings. Precise displacement measurements using diffractive gratings is an established technology (Guild, 1960), and optical encoders have been developed for precise measurements of displacement and revolution angle for a variety of applications. However, the large size and expense of conventional encoders make them unsuitable as integrated sensing devices. Recently there has been significant renewed

This work is supported by DARPA [Bio:Info:Micro] Program (MDA972-00-0032). The author wishes to thank Professor Olav Solgaard, Professor Matthew P. Scott, Dr Stefan Zappe, Dr Chung-Chu Chen, Dr Ralph W. Bernstein, Ozgur Sahin and Matthew Fish for their collaboration and helpful discussions.

Figure 1 Types of diffraction grating: (I) If arg $F = 0$, amplitude grating; and (II) If $|F| = 1$, phase grating. Where $V_0(.)$ and $V(.)$ are the incident and diffracted optical field in the α-β plane

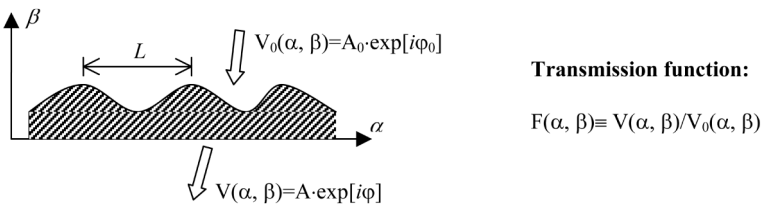

interest in using diffractive micro-optical elements as displacement sensors in atomic force microscopes (AFM) (Manalis *et al.*, 1996), accelerometer with nano-g resolution (Hall and Degertekin, 2002) and MEMS capacitive ultrasonic transducers (Loh *et al.*, 2002). For optical encoders, Sawada *et al.* demonstrated a hybrid integrated encoder with a single grating on silicon (Higurashi and Sawada, 2000). Hane *et al.* (2001) designed a dual-grating miniaturized displacement sensor using grating imaging. These advancements in microfabricated diffractive grating optics enable integrated optical encoders for sensing and microscopy of embryos and single cells.

The force encoder consists of two identical constant-period transmission phase gratings that are vertically aligned in the static state, as shown in Figure 2. When a force is applied to the needle, the upper index-grating is displaced with respect to the bottom grating. This changes the diffraction efficiency of the phase grating, and the relative position of the two gratings can be determined by the intensities in the diffraction orders. The diffraction characteristics of the dual transmission phase-grating can be analyzed by Fraunhofer diffraction theory. The first diffraction mode intensity $I_1(d)$ is a periodic function of injector displacement:

$$I_1(d) = I_0 N^2 \cdot \left(\frac{\sin c^2 \frac{Nd}{2L}}{\sin c^2 \frac{d}{2L}}\right) \times \left[(L-d)\sin c\frac{(L-d)}{4L}\right]^2 \sin^2 \phi_0 G(d) \quad (1)$$

Figure 2 (a) Solid models for optical encoder force sensor at static state (top) and the deformation of the supporting beams under central load on the force probe integrated with the index micro-grating (bottom). (b) Principle of the injection-force encoder: $2L$ is the period of the grating; $d = \text{mod}(x, 2L)$ is the displacement of the microinjector modulus $2L$; ϕ_0 represents a relative phase delay over the thickness of one grating finger

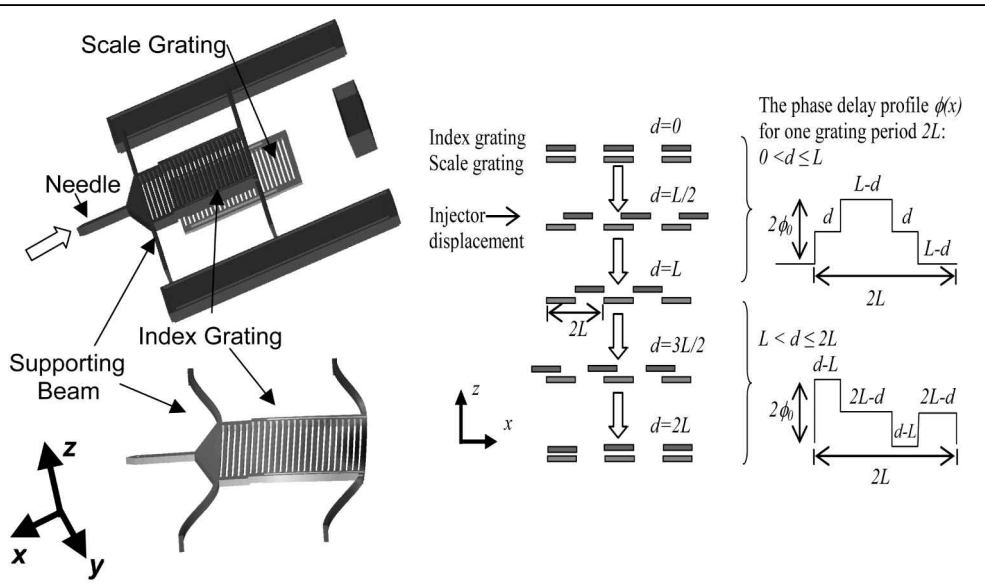

(a) (b)

$$G(d) = \begin{cases} \sin^2 \frac{\pi(L+d)}{4L} & d \in [0, L] \\ \sin^2 \frac{\pi(3L-d)}{4L} & d \in [L, 2L] \end{cases} \quad (2)$$

where I_O is the illuminating light intensity, N is the number of grating periods under illumination, $\phi_0(x) = (2\pi/\lambda)(n_1 - n_0)t$ is the phase-delay over the thickness of one grating finger, $2L$ is the period of the grating, and d is the displacement of the injector modulus $2L$.

We define the force sensor sensitivity as the change in the intensity of the first diffraction mode with respect to a unit displacement of the upper grating. The dynamic range is defined as the total range of motion over which the position can be unambiguously determined from the diffraction pattern. The trade-off between the sensitivity and dynamic range is shown in Figure 3. Encoders with larger grating period are used to have greater dynamic range, but low sensitivity (dotted line), while the opposite is true for encoders with finer pitch (solid line). For a given period, the sensitivity can be improved by increasing the number of grating periods that are illuminated, again at the cost of a reduced range (dash-dotted line). The periodicity of the encoder response can also be used to calibrate the relative displacement of the gratings.

The encoder is designed to be sensitive to translation in the x-direction, while the sensitivities to the other five degrees of freedom of motion are minimized. Translation in the y-direction can be neglected because it is small (the spring constant $k_y \gg k_x$) and has little effect on the optical readout. Likewise, rotation about the x and y axes do not affect the diffraction of the gratings and therefore can be ignored. Motion in the z-direction is also inconsequential, because the weak reflections from the grating elements lead to only small variations of the phase shift through the encoder as a function of the separation of the gratings in the z-direction. To ensure weak reflections, the grating elements must be designed such that the fields reflected from their fronts and backs interfere destructively. We achieve destructive interference by using a grating made of silicon-nitride with a refractive index of $n_1 \approx 1.9$ and a thickness of $t = 1.5\,\mu\text{m}$. Thus, the phase shift $(4\pi/\lambda)n_1 t$ associated with traversing the grating film twice is approximately an integer multiple of 2π at He-Ne wavelength $\lambda = 633\,\text{nm}$. Combined with the π phase shift of the internal reflection at the nitride/air interface, this leads to destructive interference of the two parts of the reflected field, and therefore the reflection from the grating elements is minimized. Accurate control of the film thickness can be achieved by monitored etch-back after film deposition. Silicon-nitride is well suited for our gratings, because its index allows us to minimize the back

Figure 3 Tuning of force encoder's sensitivity and dynamic range by: (I) increasing half-grating pitch period $L = L_1$ for high dynamic range; and (II) varying number of grating fingers $N = (N_2, N_3)$ for given L for local high sensitivity enhancement within $2L$ injector displacement ($L_1 = 20L_2$, $N_2 = 4N_{1,3}$)

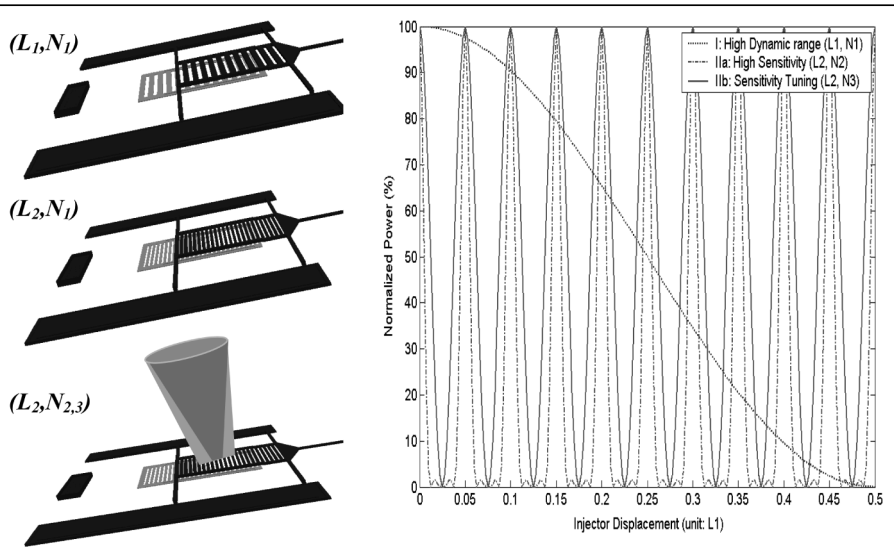

reflections and at the same time achieve a high value for the factor $\sin^2(\phi_O)$ that determines the diffraction efficiency (equation (1)). The remaining degree of freedom of motion is rotation about the z-axis. The encoder is sensitive to such rotation, so it must be minimized. The encoder therefore has maximally-separated, straight suspensions to create a large spring constant for rotation about the z-axis.

The accuracy of the force measurements depends on the spring constant k_y of the movable index grating structure. The spring constants were simulated for the geometry shown in Figure 2(a). A one-dimensional elastic model was used for the doubly-supported beam. With normally applied pressure over the two sidewalls of the probe tip, the stress and displacement vector distribution across the device were simulated using the finite element method (FEM) for supporting beams of width 8, 15 and 30 μm.

Figure 4(a)-(c) shows the scanning electron micrographs (SEMs) of the force probe and force encoder. The sensor was illuminated by a He-Ne laser (633 nm/4 mW) with spot sizes ranging from 60 to 160 μm. Figure 5 shows the measured power of the first diffraction mode as a function of absolute displacement of the injector. The grating displacement can be found from the known 20 μm period of the diffraction response. Using this calibration and a spring constant of 1.85 N/m, we find an injection force of 63 μN. The sensor as tested in Figure 5(a)

Figure 4 SEM of (a) Optical encoder force sensor. (b) Optical encoder force probe integrated with the movable index grating. (c) Index and scale gratings with 20 μm pitch and 2 μm vertical gap

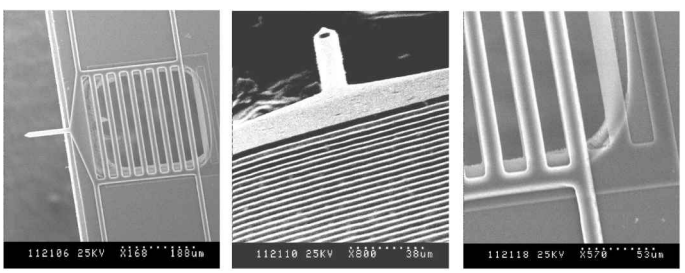

Figure 5 First diffraction mode power vs injector displacement of a force encoder with (a) $N = 10$, $L = 10$ μm and $Ky = 1.85$ N/m. The measured injection force measured: $F = 63$ μN. (b) Force sensing with a large dynamic range with $N = 3$, $L = 10$ μm and $Ky = 1.85$ N/m. The measured embryo injection force is $F = 48$ μN. Note that after the probe penetrated into the embryo, the encoder force sensor recovered back to the static state (aligned-gratings). This is shown by the sudden "jump" in the first diffraction mode power

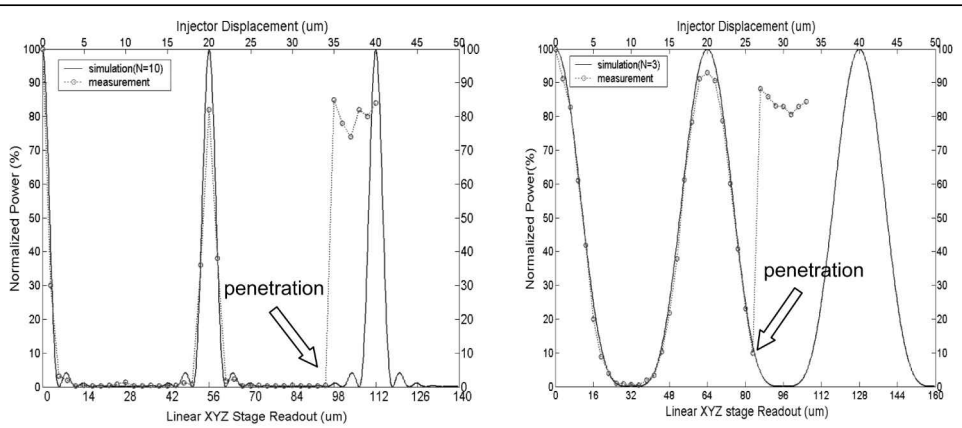

has high sensitivity around $d = 2L$, but its output is ambiguous around the displacement where penetration takes place. The solution is provided by illuminating fewer periods of the force encoder. As shown in Figure 5(b), the same force sensor illuminated by a laser spot size of 60 μm ($N = 3$), has an improved dynamic range (45 percent increase), at the cost of lower sensitivity (18 percent/μm reduction). In this case, the diffraction is not ambiguous around the penetration displacement, so both the penetration force (48 μN) and the embryo membrane deformation (57 μm) at penetration can be determined. In a series of experiments, we found an average penetration force of 52.5 ± 13.2 percent μN and an embryo deformation of 58 ± 5.2 percent μm. The measurements are in reasonable agreement with the piezoresistive-scale calibration data, demonstrating that the microencoder force sensor has sufficient sensitivity and dynamic range for monitoring injection-force dynamics in Drosophila embryos.

In the summary, we present an integrated dual diffractive micrograting-based microsurgery force sensor, with configurable sensitivity and sufficient dynamic range for monitoring penetration (thus injection) force dynamics of injections into Drosophila embryos. The application of phase modulated optical encoder approaches are shown to provide enhanced quantitative understanding of embryo microinjection dynamics in terms of fundamental membrane mechanical properties. Current work includes further downscaling design for direct probing individual cellular interactions and dynamic operation of tunable-scale probe arrays for high-throughput instrument.

References

Guild, J. (1960), *Diffraction Gratings as Measuring Scales*, Oxford University Press, Oxford.

Hall, N. and Degertekin, F.L. (2002), "Integrated optical interferometric detection method for micromachined capacitive acoustic transducers", *App. Phy. Lett.*, Vol. 80, pp. 3859-61.

Hane, K., Endo, T., Ito, Y. and Sasaki, M. (2001), "Si micromachined optical encoder based on grating imaging", *The 11th Int. Conf. on Solid-State Sensors and Actuators*, 10-14 June 2001, Munich, Germany.

Higurashi, E. and Sawada, R. (2000), "High-accuracy micro-encoder based on the higher-order diffracted light interference", *Int. Conf. on Opt. MEMS*, 21-24 August 2000, Hawaii.

Lal, A. and White, R.M. (1995), "Micromachined silicon needle for ultrasonic surgery", *IEEE Ultrason. Sym.*, pp. 1593-5.

Loh, N., Schmidt, M.A. and Manalis, S.R. (2002), "Sub-10 cm^3 interferometric accelerometer with nano-g resolution", *J. Microelectromech. Sys.*, Vol. 11 No. 3, pp. 182-7.

Manalis, S.R., Minne, S.C., Atalar, A. and Quate, C.F. (1996), "Interdigital cantilevers for atomic force microscopy", *Appl. Phys. Lett.*, Vol. 69 No. 25, 16 December 1996.

Sharp, P.A. and Zamore, P.D. (2000), "RNA Interference", *Science*, Vol. 287, p. 2430.

Zappe, S., Zhang, X.J., Bernstein, R.W., Furlong, E.M., Fish, M., Scott, M.P. and Solgaard, O. (2002), "Micromachined hollow needle with integrated pressure sensors for precise, calibrated injection into cells and embryos", *The Sixth Int. Sym. on Micro Total Analysis System (μTAS)*, 3-7 November 2002, Nara, Japan.

Zhang, X.J., Zappe, S., Bernstein, R.W., Sahin, O., Chen, C-C., Fish, M., Scott, M. and Solgaard, O. (n.d.), "Micromachined silicon force sensor based on diffractive optical encoders for characterization of microinjection", *Sensors and Actuators*, Phy. A (SNA4047, in press).

Zhang, X.J., Zappe, S., Bernstein, R.W., Sahin, O., Chen, C-C., Scott, M. and Solgaard, O. (2003), "Integrated optical diffractive micrograting-based injection force sensor", *Proc. Int. Conf. on Solid State Sensors and Actuators*, (Transducers'03), Boston, USA, pp. 1051-4.